

ATI NO. 164174  
ASTIA FILE COPY

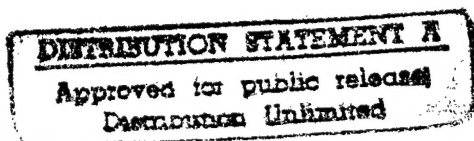
STI

UNITED STATES ATOMIC ENERGY COMMISSION

AECU-1853

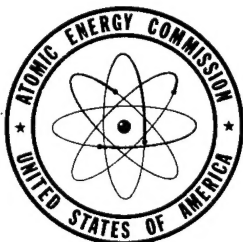
ELECTRON RADIOGRAPHY

By  
Arthur I. Berman



December 5, 1950

Los Alamos Scientific Laboratory



ETHIC QUALITY INSPECTED 2

Technical Information Service, Oak Ridge, Tennessee

19961101 075

## ABSTRACT

Electron radiography is considered both theoretically and empirically as a method of analysis essentially of (1) thin biological sections, and (2) polished metallurgical surfaces. Comparative illustrations are shown of this and complementary techniques using soft X rays and visible light; the scope and limitations of each are cited.

## PHYSICS

Reproduced direct from copy  
as submitted to this office.

PRINTED IN USA  
PRICE 20 CENTS  
Available from the  
Office of Technical Services  
Department of Commerce  
Washington 25, D. C.

This report is based on LADC-993.

# ELECTRON RADIOGRAPHY

Arthur I. Berman

## CONTENTS

	Page No.
I. Introduction	4
II. Ejection of Electrons by X Rays	5
A. Photoelectric Absorption	5
B. Compton Effect	8
C. Direction of Ejection	11
III. Electron Interactions	14
A. Absorption	14
B. Scatter	16
IV. Transmission Electron Radiography	18
A. Comparison with X Radiography and Photography	18
B. Best Techniques	22
V. Back Emission Electron Radiography	28
A. Best Techniques	28
B. Factors Affecting Photographic Density	30
VI. Summary	32

## I. INTRODUCTION

The two techniques of electron radiography have been considered previously.<sup>1</sup> They are: (1) thin-specimen radiography using fast electrons as radiation rather than soft X rays; (2) surface electron emission (usually from metallurgical subjects) upon a photographic plate.

In (1), called 'transmission electron radiography', a thin foil of a heavy element, e.g., lead, is pressed in contact with a specimen and a fine-grain emulsion. Hard X rays incident on the foil eject electrons, some of which go through the specimen to the emulsion, exposing it in amounts depending upon the energy and number of the electrons which have penetrated the specimen. Figure 1 A schematically illustrates the arrangement for this technique.

In (2), called 'back emission electron radiography', a polished surface is placed in direct contact with a fine-grain emulsion in such a manner that hard X rays pass through the emulsion and eject electrons from the specimen surface. The emulsion is exposed in amounts depending mainly on the atomic numbers of the surface elements in contact with it. The experimental arrangement for this technique is shown in Figure 1 B.

The principal advantage of (1) over X radiography is that a standard high-voltage X-ray unit may be used for thin-specimen radiography if a low-voltage, high-intensity, minute focal spot unit is unavailable. Furthermore, the radiographs are dissimilar--electron transmission is influenced essentially by physical density

changes, whereas low-voltage X-ray transmission is highly sensitive to atomic number differences. The advantage of (2) over photographic analysis is that surface components which may be indistinguishable by visible light might easily be differentiated, without the necessity for etching, because of the difference in the numbers of electrons per unit area which may be ejected; in addition, this method may permit identification of the components.

It is the purpose of this paper to extend the treatment of these two methods in order to arrive experimentally at the best conditions of exposure, quality of radiation, type of emulsion, etc. Included also is a short theoretical discussion of electron emission, absorption, and scatter in order that the mechanism may be understood and the results applied in practice. The limitations of these techniques, as well as useful applications, are noted.

## II. EJECTION OF ELECTRONS BY X RAYS

When X rays with less than one million electron volts of energy pass through matter, their source of energy loss, or absorption, is electron interaction. Two processes are present: (A) photoelectric absorption and (B) the Compton effect.

### A. Photoelectric Absorption

In this process, the X-ray quantum is completely absorbed. Part of its energy is used to remove an electron from an atom and the remainder is present as kinetic energy of the electron.

This 'photoelectron' kinetic energy may be written:

$$m_0 c^2 \left[ \left[ 1 - (v/c)^2 \right]^{-\frac{1}{2}} - 1 \right] = \frac{m_0 v^2}{2} \left( 1 + 3v^2/4c^2 + \dots \right)$$

$$= h\nu - W_n,$$

where:  $m_0$  is the electron rest mass,

$v$  is its emergent velocity,

$c$  is the velocity of light,

$h\nu$  is the energy of the incident quantum

( $h$  = Planck's constant and  $\nu$  is the frequency of the incident quantum), and

$W_n$  is the electron binding energy at the particular atomic shell,  $n$  ( $n = 1, 2, 3, 4$  -----), from which the electron is removed.

When  $v \ll c$  the kinetic energy reduces to the more familiar  $\frac{1}{2} m_0 v^2$ .  $W_n$  is proportional to  $(Z - a_n)^2 / n^2$  where  $Z$  is the atomic number and  $a_n$  is a constant ( $a_n < Z$ ) depending on  $n$ . Thus, an electron in the innermost shell ( $n = 1$  or K shell) is bound with an energy of about  $R(Z - 1)^2$  where  $R$  is constant (about 13.5 electron volts). The L and M shells follow, in which electrons are bound with energies approximately  $R(Z - 5)^2 / 4$  and  $R(Z - 13)^2 / 9$  respectively.<sup>2</sup>

Considerations of energy and momentum balance indicate that it is impossible for a free electron to absorb a quantum (although it may scatter one). The probability of electron ejection is greatest for most highly bound electrons. In fact, experiments performed near 500 kilovolts X-ray energy indicate that the K shell alone accounts for about 80 per cent of the total photoelectric atomic absorption.<sup>3</sup> This is also close to the result of theoretical calculations, and therefore, following Heitler<sup>4</sup>, it will be assumed that the total photoelectric absorption is  $5/4$  that of the K-shell

absorption. The atomic cross section for the photoelectric emission of an electron in the K shell of an atom increases rapidly with atomic number (proportional approximately to  $Z^5$ ). The absorption coefficient is proportional to the K cross section per atom times the density of atoms in the material. This density varies from element to element but remains, for most of the common metals, with few exceptions, close to the value  $(5 \pm 3) \times 10^{22} \text{ cm}^{-3}$ . Typical values are: aluminum-- $6.0 \times 10^{22} \text{ cm}^{-3}$ , iron-- $8.5 \times 10^{22} \text{ cm}^{-3}$ , tungsten-- $6.3 \times 10^{22} \text{ cm}^{-3}$ , and lead-- $3.3 \times 10^{22} \text{ cm}^{-3}$ .

If X rays enter a semi-infinite volume, then the number of photoelectrons produced between depth  $x$  and  $x + dx$  is

$$dN_e = k_1 I_x N \sigma dx$$

where:  $I_x$  is the incident intensity at  $x$ ,

$N$  is the number of atoms per  $\text{cm}^3$  ( $= N_0 \rho / A$  where  $N_0$  is Avogadro's number,  $\rho$  is the physical density, and  $A$  is the atomic mass),

$\sigma$  is the cross section per atom for the photoelectric effect, and

$k_1$  is a constant.

The number of photoelectrons from within this volume which reach the incident surface,  $N_s$ , will be proportional to

$$k_1 N \sigma \int_0^R I_x dx$$

where  $R$  is the electron range in the material. Since  $R$  is small in comparison with the 'radiation length' (reciprocal of absorption coefficient) of the X rays, one may write  $I_x = I_0$ ,

and

$$N_s = k_2 N \sigma R.$$

But  $R$  is inversely proportional to the electron density,  $NZ$ , because the electrons in the volume provide most of the stopping power (see Section III A). Whence,

$$N_s = k_3 \sigma / Z.$$

Because  $\sigma$  is proportional to  $Z^5$ , one finds, therefore,

$$N_s = k_4 Z^4.$$

From this relation, it might be inferred that, in practice, the photographic density observed at the surface of an absorber will be a simple function of atomic number and that this effect could be used as a qualitative analysis of elements. The actual photographic density present, however, depends upon such factors as (a) the fraction of scattered radiation present (see next section), (b) the value of the K-absorption limit, (c) the response of the emulsion to energy of the electrons, and (d) the thickness of the particular sample chosen.

#### B. Compton Effect

In the Compton effect the photon interacts with an electron of negligible binding energy, the event being interpreted in terms of simple mechanical laws of elastic collision. From the conservation laws it follows that the photon is scattered with lower energy  $h\nu'$  ( $\nu' < \nu$ ), the excess being taken up by the electron. These Compton electrons, or recoil electrons, are always emitted in the forward hemisphere and hence are useful in transmission electron radiography, whereas their importance in the back emission radiographic process is restricted to back-scatter effects.



A distinction may be made in the Compton process between absorption and scattering: The total Compton effect electronic cross section in  $\text{cm}^2$ , found theoretically by Klein and Nishina, gives a measure of the probability for a quantum-free-electron interaction to occur. Multiplying by the electron density yields the total Compton coefficient in  $\text{cm}^{-1}$ . From this coefficient the fraction of quanta scattered by electron interactions may be found for any thickness of material. One may distinguish between a Compton scattering coefficient and Compton absorption coefficient, because the quanta are scattered at lower energy and the difference is absorbed by the electrons as kinetic energy. The sum of the coefficients is called the total Compton coefficient. In the photoelectric process the quantum is completely absorbed and the associated coefficient is often called 'true' absorption; however, the Compton effect also may contribute much to the 'true' absorption except at low X-ray energies.

For thicknesses small in comparison with the radiation length, the total Compton coefficient is directly proportional to the ratio: scattered quanta/incident quanta; likewise the photoelectric coefficient is proportional to: photoelectrically absorbed quanta/incident quanta. A Compton electron is associated with each scattered quantum, and a photoelectron with each 'photoelectric quantum' (neglecting the low-energy Auger electrons, see below); hence the ratio: number of Compton electrons/photoelectrons equals total Compton coefficient/photoelectric coefficient. This was verified for air by Compton and Simon.<sup>5</sup>

At 250 kilovolts primary energy, the Compton coefficient is more than seven times the photoelectric coefficient for all elements below iron and is equal to the photoelectric coefficient for silver. For the heavy elements (e.g., lead) the Compton coefficient is only about 20 per cent of the photoelectric coefficient. At 150 kilovolts the Compton coefficient lags behind the photo coefficient above arsenic, and at lead it is only 5 per cent of the latter. Figure 2 illustrates the variation of the photoelectric to Compton coefficient ratio for lead and aluminum in the 100 to 1000 kilovolt range.

It is seen, then, that for heavy element absorbers the largest number of electrons emitted near the 200 kilovolt X-ray region are photoelectrons. For the light elements, recoil electrons predominate (especially at high incident energies) and Compton X-ray scattering provides significant background intensity which may produce even greater film density than the electrons from the absorber. At primary X-ray energies of the order of 200 kilovolts and above, all secondary emissions as well as primary processes, are predominantly in the forward hemisphere.

When a photoelectron is emitted and the atom is left in an excited state, it will return to its normal state often with the ejection of a quantum, or several quanta, of relatively soft (below 100 kilovolts) fluorescent radiation. Usually the excited atom will emit other electrons, called Auger electrons.

To summarize, when X rays of, e.g., 200 kilovolts energy enter a high atomic number material, many photoelectrons are

ejected, together with much fluorescent radiation, some Auger electrons (which are absorbed very readily), some Compton-scattered radiation, and Compton electrons. When these primary quanta enter a low atomic number material, relatively much Compton-scattered radiation and many Compton-scattered electrons, moving in the forward hemisphere, are present. There are relatively few photoelectrons with their accompanying fluorescent radiation and Auger electrons. Furthermore, the ratio of the occurrence of the photoelectric effect to the Compton effect decreases for both low- and high-atomic numbered elements as the primary radiation energy increases. It would be most desirable to choose a material and operating energy, for electron radiography, where this ratio is relatively high, to increase the supply of photoelectrons (despite the presence of some disturbing low energy fluorescent radiation) relative to the Compton scatter background (see Figure 2).

#### C. Direction of Ejection

The main secondary process in electron radiography is photoelectric emission (because the X-ray operating energy which yields best general results is in the region of 250 peak kilovolts as noted in Section IV B, and the materials used as emitters are high in the periodic table); therefore, it is worthwhile to consider the intensity distribution of these electrons with respect to the incident quantum direction. Reference to Figure 3, taken from Heitler<sup>6</sup>, indicates that they are emitted mainly at right angles to the X rays. At low energies the differential cross section follows a  $\sin^2\theta$  law where  $\theta$  is the angle between the emitted electron and the

incident quantum. If the kinetic energy of the electron is of the same order of magnitude as, or greater than, its rest mass energy,  $m_0c^2$  ( $\sim 0.5$  Mev), then a relativistic correction should be applied which displaces the distribution in a forward direction as shown in Figure 3. The differential cross section is then written:<sup>7</sup>

$$\sigma d\theta = k \sin^2\theta d\theta / (1 - \beta \cos\theta)^4$$

where  $\sigma$  is the cross section,  $k$  a constant, and the denominator includes a relativistic correction term ( $\beta \equiv v/c$ ). For a 200 kilovolt electron the correction term is definitely not negligible, since  $\beta = 0.7$ .

One may determine the proportionate number of electrons back-emitted perpendicular to a photographic plate, in contact with the emitter, and inclined at an angle  $\varphi$  to the X-ray direction (see Figure 4). Because the intensity of primary X rays striking the emitting surface is proportional to  $\sin\varphi$ , the intensity in the  $\theta$  direction is

$$I_\theta = I_0 \sin^2\theta \sin\varphi / (1 - \beta \cos\theta)^4,$$

$$\text{but since } \cos\theta = -\sin\varphi \text{ and } \sin\theta = \cos\varphi,$$

$$I_\theta = I_0 \cos^2\varphi \sin\varphi / (1 + \beta \sin\varphi)^4.$$

To find the value of  $\varphi$  which will make  $I_\theta$  maximum,  $dI_\theta/d\varphi$  is set equal to zero, obtaining  $\beta \sin^3\varphi - 3 \sin^2\varphi - 3 \beta \sin\varphi + 1 = 0$ . Solving this cubic equation for  $\varphi$  when  $\beta = 1$  (extreme relativistic case), results in  $\varphi = 15.5^\circ$ , and when  $\beta = 0$  (non-relativistic case),  $\varphi = 35^\circ$ . Since electrons always have a value of  $\beta$  between 0 and 1, a maximum density will be produced in a plate inclined at some particular angle  $\varphi'$ , between  $15^\circ$  and  $35^\circ$ , assuming the electron direction is not changed after

it leaves the atom. In principle one could determine the effective energy of the emitted electrons by observing the angle of maximum density when the plate is tilted with respect to the direction of the X rays through various values of  $\varphi$ .

When this experiment was performed, however, it showed that, within limits of experimental error, the density present on the photographic plate when  $\varphi$  is  $90^\circ$  is actually slightly greater than when  $\varphi$  is between  $15^\circ$  and  $35^\circ$ . This experiment was repeated after placing a lucite pinhole collimator  $1/16''$  thick between the emulsion and emitter, and similar results were obtained.

This fact is significant because it illustrates the tremendous amount of internal electron scattering (discussed further in Section III B) that must be present within the emitter itself. It is this scatter which permits a large amount of surface electron emission in the direction opposite to that of the incident X rays, even though, as seen in Figure 3, there should be zero emission in this direction.

Scattered and fluorescent radiation will, of course, account for some of the photographic density, but still nearly all of it must have been caused by electrons, for an intervening cellophane filter reduces the blackening to a small fraction of its former value. Thus, the plate can be placed perpendicular to the X rays and the maximum X-ray flux may be utilized; this also assures essentially constant X-ray flux over the surface of the plate when it is close to the source.

The most unfavorable effect of this electron scattering is the low degree of resolution that characterizes electron

microradiographs in comparison with photo and X-ray micrographs. Were it not for certain special advantages, electron radiography would be of no value as a supplement to these other techniques.

### III. ELECTRON INTERACTIONS

#### A. Absorption

Electrons, in traversing matter, experience two general types of interaction: elastic collisions, or scattering, and inelastic collisions, or absorption. Scattering will be discussed in the next section for its influence in electron radiography.

Inelastic collisions with atomic nuclei account for some small fraction of the energy loss of electrons. The electron is deflected by the nuclear Coulomb field and the resulting acceleration produces X radiation. This is the origin of the continuous spectrum (or bremsstrahlung) in the target of X-ray tubes. Fortunately, the probability for the occurrence of this process is relatively small at the energy range encountered in electron radiography; otherwise additional X-ray background would be present in all electron radiographs.

Most of the energy lost by an electron traversing either the emitter, the specimen, or the emulsion itself, is by inelastic collisions with atomic electrons. In this process the interacting electric forces separate the atomic electron from its parent atom and an ion pair is produced. The amount

of energy lost by the moving electron in each collision equals the binding energy of the atomic electron plus the kinetic energy which it receives. The lost energy per unit path length is directly proportional to the electron density of the matter traversed:  $N_0 \rho Z/A$  (see Section II A). Since  $Z/A$  remains fairly constant through the periodic table, decreasing very slowly as  $Z$  increases, one can state that the electron density is approximately proportional to the physical density. Thus, the range of electrons of a particular energy often is given, not in terms of thickness, which varies from element to element, but in the unit  $\text{g/cm}^2$ --the product of thickness and density--which is nearly of the same value for all elements.

In Figure 5, an empirical curve is shown of electron range, in the unit:  $\text{mg/cm}^2$  of aluminum, for energies up to 350 kilovolts.<sup>8</sup> An approximate value (within about 20 per cent) of the range in centimeters in any element can be found by dividing the value on the curve by the density in  $\text{mg/cm}^3$ . Thus, from the curve, the range of 200 kilovolt electrons is  $40 \text{ mg/cm}^2$ , or  $0.148 \text{ mm}$  in aluminum,  $0.045 \text{ mm}$  in copper, and  $0.035 \text{ mm}$  in lead. The theoretical range values were given by Heitler<sup>9</sup> for air (at normal temperature and pressure), water (similar to soft biological tissue), and lead. From these data curves have been drawn of the range in centimeters from 50 kilovolts to 500 megavolts for these three materials and are shown in Figure 6. It is evident that the electron range is considerably larger than the empirical value. This is due to multiple scattering--a tortuous path is followed

through the material; thus, the integral of the path length is several times longer than the net stopping distance in the initial electron direction. When most of the energy is dissipated, the electron diffuses through the medium by random motions; however, this is of little consequence in electron radiography.

One would expect a continuous spectrum of electrons because of the continuous character of the primary X radiation; the absorption curve resembles that of Figure 7. The intensity transmitted is an exponential function of thickness for most of the curve, until the value of maximum range is reached at which negligible energy remains.

#### B. Scatter

Because the absorption curve of electrons is somewhat similar to that of low-energy X rays, one might expect the same contrast and detail present in transmission electron radiographs as is obtained in low-voltage X radiographs. In reality, however, the two results are quite different.

The difference lies in the nature of absorption. When low-voltage X rays enter a medium they are 'truly' absorbed, which means that all the quantum energy is removed and is ultimately present in the material in inactive forms such as heat (except for a low background of fluorescent radiation). Electrons, on the other hand, are severely scattered primarily by atomic nuclei; although diverted from their original path, the electrons often reach the film (see Section II C). The resulting electron radiograph is diffused and of low contrast, similar to the high-energy X radiograph obtained



when a thick low-density material in which Compton scatter effects are so pronounced is radiographed.

If an unfiltered beam of X rays, excited by 200 peak kilovolts, impinges on a plate of aluminum, experiment shows<sup>10</sup> that complete electron absorption occurs with about 20 mg/cm<sup>2</sup> of aluminum. Thus, the absorbed electrons have an average energy of 120 kilovolts. A negligible number of these electrons have energies of 200 kilovolts; the X rays are inhomogeneous and the electrons are absorbed at different depths. After adjusting the empirical range curve for lead, it may be concluded that no electrons originate deeper than about 0.0018 cm below the lead surface for the same quality of X radiation. The effect of scattering in a thickness of lead equal to this may be calculated.

From an elementary theory of electron scattering in thin foils<sup>11</sup>, it is found that the most probable angle of deflection,  $\Theta$ , is approximately proportional to the atomic number and inversely proportional to the kinetic energy, for high energies. For lead  $\Theta$  is about  $2.5 \times 10^4 D^{1/2} / E$ , where D is the thickness in centimeters and E is the initial kinetic energy in kilovolts. Assuming that this formula holds for 120 kilovolt electrons, they would thus be deflected about eight radians while passing through 0.0018 cm of lead.

This huge value of the deflection angle, and the fact that relatively few electrons are ejected directly forward or backward from the atom, emphasizes the futility, in electron radiography, of expecting the desired parallel beam of electrons to stream toward the sensitized surface. In back

emission radiography this means that electrons which emerge from within the specimen in considerable numbers will diffuse the surface image. In transmission radiography this means that electrons will emerge from the radiating foil in random directions (further scattered even by a low atomic number specimen) and will severely impair the resolution of the image.

#### IV. TRANSMISSION ELECTRON RADIOGRAPHY

##### A. Comparison with X Radiography and Photography

In Figure 8, prints of an X radiograph, a transmission electron radiograph, and a transmission photomacrograph of a 25 micron section of rat tooth, enlarged 4.5X, are shown together for comparison. Figure 8 A is a positive reproduction of an Eastman 649-GH spectroscopic plate exposed to X rays emanating from a tungsten-target, 1.5 mm projected-square focal spot tube operated at 8 peak kilovolts and 25 milliamperes, for 15 minutes at 25 cm from the plate. The X rays were filtered by the beryllium tube window, air, and an infra-red gelatin filter (Wratten 87) which permitted operation of a 'vacuum cassette'. In this device atmospheric pressure forces the filter tightly against the specimen and emulsion. Plates were developed seven minutes in Vonel S-35 physical developer as a standard for all radiographs in this paper. Figure 8 B is a positive reproduction of a plate exposed essentially by electrons ejected from a 25 micron lead foil with X rays from a tungsten-target tube, 30 cm

distant, excited at 250 peak kilovolts. To insure the best possible contact, a vacuum cassette was again employed, with opaque, flexible vinylite replacing the infra-red filter. Exposure was 4 minutes, at 15 milliamperes, with filtration of 3/16 inch copper and 3/16 inch aluminum (see next section). Anomalous cracks are due to splitting of this thin specimen and separation from the gelatin mount. Figure 8 C is a transmission photomacrograph print of the same specimen.

The contrast between regions differing in composition is more pronounced in either radiograph than in the photomacrograph, regardless of light absorption properties. (Notice the difference in contrast between the central portions lacking calcium and the surrounding calcified tissue.) The photographic view, on the other hand, while not revealing this, delineates overall structural details well.

The maximum resolution obtained with these methods may be mentioned here. Minimum resolvable distance is defined as the smallest distance between two points which may still be distinguished as such in the image. A term frequently used incorrectly is maximum permissible magnification. The minimum resolvable distance of two points, viewed at a normal distance (about 25 cm) by the human eye, is usually defined arbitrarily as 0.1 mm. For example, when a micrograph is enlarged 100X until the most closely spaced image points are just 0.1 mm apart, the maximum unit of enlargement permissible for that particular specimen, emulsion, and optical system is said to be 100X. Further enlargement will reveal no additional detail.

The finest-grained emulsions available (e.g., Lippman emulsion or Eastman spectroscopic plates) can theoretically resolve points one micron apart. An enlargement of 100X is thus possible before the image of these points is separated by 0.1 mm. Again, additional enlargement will result only in a diffused image.

If microradiographs of ultra-thin specimens are made, while maintaining good contact with the emulsion, with X rays emanating from a minute focal spot far from the film, the resolution is limited solely by the grain size of the emulsion, permitting about 100X magnification, as mentioned above. From geometrical considerations, it can be shown that even with a specimen 0.1 mm thick in contact with the emulsion and at 15 cm from a 1.5 mm focal spot, the resolution is still limited by emulsion grain size alone. The grain size appears not to be influenced by the mode of exposure, be it X rays, electrons, or visible light.

In Figure 9 A a section of the same specimen, taken at 8 peak kilovolts is shown magnified 25X directly from the plate (and therefore is reversed in density with respect to Figure 8). In an effort to increase the contrast still further, a 6.5 peak kilovolt exposure was made, shown in Figure 9 B. This constitutes almost the practical minimum of X-ray operating voltage. Because of excessive X-ray attenuation by the gelatin filter the vacuum cassette had to be abandoned, resulting in a loss of definition caused by poor contact. Furthermore, the low-energy tube output necessitated 90 minutes exposure time. Space charge limited the tube current to 20 milliamperes.

By comparing the X radiographs with the 250 peak kilovolt electron radiograph of Figure 9 C, definite conclusions can be reached which agree with the theory presented in the previous sections:

(1) Maximum contrast between components differing in their chemical composition can be obtained with X rays. Photoelectric absorption, which accounts for nearly all primary beam attenuation at low voltages, varies approximately with the fourth power of atomic number, except at absorption discontinuities; therefore, slight differences in atomic number are revealed as large differences in photographic blackening. Generally, as lower voltages are attained, this effect is enhanced. The reason is that the absorption coefficient of nearly every element increases, as the energy decreases, so that the difference in intensity transmitted by two elements becomes greater, for a given thickness, at low voltages. In both X radiographs, a marked difference between the calcified and non-calcified tissue is revealed--at the expense, however, of detail in both the light and dark regions.

(2) On the other hand, electrons are sensitive principally to density differences in the material being radiographed; they are absorbed essentially without respect to atomic number. Thus, density changes are delineated as gradations in emulsion density in both low and high atomic number regions. The small white spots, revealed best in the electron radiograph, for

the reasons above, represent holes in the specimen, which may be interpreted as a change in density, from tissue to air, the spacing between emitter and emulsion being constant.

For the examination of thick sections, electron radiography becomes far inferior to X radiography and photography because of the electron scatter-absorption problem discussed in the last section. In Figure 10 the three processes again are compared; the specimen is a baby mouse skull section with plutonium deposits, the thickest part being 125 microns, or five times the thickness of the rat tooth specimen. Parts A, B, and C were made under conditions identical with the corresponding parts of Figure 8, except that the operating potential for the X radiograph was 12 peak kilovolts and the exposure time 2 minutes.

In the thicker portions of the specimen electrons are completely absorbed, and it is only in the thinner regions that electron scattering and absorption are low enough to permit some measure of detail. The background density is mainly a result of the presence of fluorescent and scattered radiation. Significantly, both radiographic methods permit differentiation between the plutonium-impregnated bone tissue and its surroundings to a degree that is not achieved with visible light.

#### B. Best Techniques

A study was undertaken to determine the techniques most satisfactory in transmission electron radiography. The results

are discussed below:

(1) Filtration:

It is apparent that soft X rays must be prevented from reaching the sensitive surface as they contribute to only the background density, producing negligible photoemission. The result of filtering the beam with a thick plate of almost any material is shown in Figure 11. Because of the dependence of X-ray absorption on wavelength in all elements, very hard X rays (of short wavelength) are reduced only slightly in intensity, while soft X rays are absorbed almost entirely (by photoelectric absorption).

For electron radiographs taken with the tube operating at 250 kilovolts or below, the filter consisted of 3/16 inch of copper plus 3/16 inch of aluminum. The aluminum was added to absorb characteristic fluorescent radiation and Compton scatter from the copper. When this total filtration was doubled, the background density was reduced very slightly but the exposure was increased about four times to maintain the density at the previous value. It was felt that an increase in filtration was not essential. Decreasing the amount of filtration shortened the exposure time but introduced what was considered to be excessive background density.

(2) Emulsion:

Although the ultra-high resolution property of spectroscopic plates is not essential, it was found that they are the most satisfactory of all plates and films

tested. Their background density is much lower than any other, and exposures required are only a few times that for 'fast' coarse-grained films. This may seem somewhat odd, as the sensitivity of these thin-emulsions plates to X rays is 50 to 100 times less than, for example, Eastman Kodak Industrial Type M X-ray film. Yet the relative electron sensitivity in the spectral plates is not nearly as low (the relative speed factor is about five). This may be explained by the fact that in a thick emulsion the X-ray energy lost is much greater than in a thin emulsion. Electrons, on the other hand, may lose nearly all of their energy in either emulsion, because of their short range.

Thus, the spectroscopic plate, though considered as having very low sensitivity, still produces high-contrast electron radiographs at fairly short exposure times, retaining also the fine-grain property. Eastman 649-GH and 548-0 plates were tested and each was found to be satisfactory for electron radiography; the latter was slower but provided slightly higher contrast. A second good medium proved to be Kodak orthochromatic film<sup>12</sup>, which provided relatively low background and good electron sensitivity but did not yield radiographs of quite as high quality as the plates.

### (3) Quality of the Primary X Radiation:

In Figure 12, comparison electron radiographic prints of the mouse skull and rat tooth specimens of Figures 8 and 9 are shown, made with electrons ejected



from a 1 mil lead foil by X rays from tubes operated at 150, 250, and 1000 peak kilovolts respectively. The X rays were filtered by 3/16 inch copper and 3/16 inch aluminum at the first two voltages and 3/8 inch copper in the last. The 250 peak kilovolt exposure was one-fourth as large as at 150 peak kilovolts; both were taken with the same X-ray unit. The best operating voltage, from all standpoints, seemed to be 250 peak kilovolts. The 150 peak kilovolt exposure still compares favorably, but penetration is not as deep. At 1000 peak kilovolts the increased proportion of scattered X rays emanating from within the lead foil may account for the loss of detail in the third print. Because of the slight absorption of very high-energy electrons by thin specimens, the results of experiments performed with the Los Alamos radiographic betatron proved unsuccessful.

(4) Emitter:

Lead seems to be the most satisfactory electron-emitting material because of its high atomic number, high electron density, and its ability to mold about the specimen in tight contact without damaging it. There seemed to be no marked difference in electron emission using other dense materials such as tungsten and gold. When a low atomic number material, e.g., nickel, was used as emitter, contrast was reduced because of the X-ray background, and no increased resolution was observed. No gain in quality was apparent by increasing the lead thickness from 25 microns

to 50 or 75 microns. The only effect noted was the absorption of the primary X rays to a greater degree, necessitating longer exposures.

Figure 13 illustrates an interesting application of electron transmission radiography. A piece of typed bond paper was photographed by transmitted light, as shown in Figure 13 A. This same paper, when electron-radiographed at 250 peak kilovolts, shows no trace of typing (Figure 13 B). This is true whether the typed or untyped side of the paper faces the emulsion. Again the absorption process provides the solution to this paradox. The carbon in the typing blends with the organic compounds in the paper, and, being apparently of almost equal density, is not differentiated by the electrons. The density (or thickness) change in the watermark, however, is easily distinguished. The typing is discernible in the light, for light absorption is not solely a function of density. A low-voltage X radiograph (not shown) clearly reveals the typing because, as discussed before, the absorption process is photoelectric and extremely sensitive to atomic number differences.

The results described above may be reversed when other specimens are used: Components which appear identical under visible light might easily be separated by electrons (as already noted in Figure 8).

In Figure 14 another use of electron radiography is illustrated. Pictured in Figure 14 A is a transmission electron radiograph of black paint coated on a nickel base,

taken with 250 peak kilovolt X-ray-excited electrons back-emitted from the nickel and through the paint (magnification: 3X). The experimental arrangement is described essentially in Figure 1 B. It is probable that some small amount of fluorescent and scattered radiation also contributed to the radiograph, as well as electron radiation from the paint itself. A visible light photograph of the paint coat is shown for comparison in Figure 14 B. While the light visualizes surface deformations, electrons reveal the internal structure of the paint coat.

It may be asked whether transmission radiographs made by back-emitted electrons in this manner are of the same quality as the radiographs made by electrons moving in the same direction as the primary X rays. Experiment indicates that the quality obtained with the latter technique is far superior and the former method is not recommended unless it is the only one practicable.

It might be mentioned that the method of electron radiography described in this paper is not limited to X-ray excitation, and the elaborate equipment which it entails. For example, it is perfectly feasible to coat a beta-emitting isotope on a flat, heavy base and take transmission beta radiographs on either the same sensitive type of plate considered, or a faster one, since a gamma-ray background may be absent. The simplicity of this method makes it extremely useful in the biological laboratory, although, of course, long exposure times may be required.<sup>13</sup>

## V. BACK EMISSION ELECTRON RADIOGRAPHY

### A. Best Techniques

It was found that many of the results described above apply equally well to back emission electron radiography. Filtration to eliminate the X-ray background is especially important since the exciting X rays must first pass through the emulsion before ejecting the photoelectrons. The numerical value of exciting voltage for good resolution seems not to be critical, but at voltages which are very high the photo-emission cross section decreases considerably, reducing contrast. At very low operating potentials, the high absorption by the emulsion of the soft primary and fluorescent X rays will fog the film. A good operating voltage for general work seems to be 250 peak kilovolts, for at this value, with sufficient filtration, the background density is low, resolution and contrast are good, and exposure times are reasonably short. Filtration again is set at 3/16 inch copper and 3/16 inch aluminum.

Figure 15 shows a 3X enlarged photomacrograph and positive reproductions of back emission electron radiographs taken at 250 peak kilovolts (Figure 15 A) and 1000 peak kilovolts (Figure 15 B) of the polished surface of a gold aluminum alloy specimen. The photomacrograph (Figure 15 C) obviously delineates greatest detail; but, in general, one could not identify the elements and be sure, for example, which was the gold--while either electron radiograph leaves no doubt.

As noted in Section II C, no electrons are ejected from the atom exactly in the direction of the X-ray source. Hence, one must depend upon scattered electrons alone to make the radiograph, and enlargements of more than 15X apparently are impossible without encountering serious diffusion. Figure 16 is a 15X enlargement made directly from a portion of the plate taken at 250 peak kilovolts (and is reversed in density with respect to Figure 15). Good contact between specimen and emulsion is indispensable, and in many cases a fine polish on the surface is essential for sharp images. The slight fuzziness of the central regions of the electron image results from lack of a polished surface. The vacuum cassette again is used whenever practicable.

It was stated in a previous paper<sup>14</sup> that magnifications of 'many thousands of times', using Lippman emulsions, could be made of electron back emission radiographs. This seems to be unlikely if the writer is assuming magnification in diameters, and if normal viewing distance is implied.

It might be argued that perhaps a technique would be practicable in which the relative position of the surface and emulsion might be reversed with respect to the incident X rays so that the rays may first penetrate the specimen and eject photoelectrons in a forward direction which, at the specimen surface, will strike the emulsion and produce somewhat sharper radiographs. This is not satisfactory usually, because the specimen itself absorbs the X rays and reduces their intensity.

Figure 17 is a 3X enlarged back emission electron radiograph print of the surface of a lead-plastic bonded material (Durez). The surface corresponding to Figure 17 A was rejected by electron back emission inspection because of the inhomogeneity of the mixture, the black spots indicating concentrations of lead. Figure 17 B, however, reveals an excellent surface.

#### B. Factors Affecting Photographic Density

It was mentioned in Section II A that the technique of back emission electron radiography was anticipated as a possible means for qualitative absolute determinations of elements. Experiments performed have discounted this possibility despite the sensitive atomic number dependence of the photoelectric effect.

The following elements were set upon a rubber base: aluminum, nickel, copper, molybdenum, tin, tungsten, gold, lead, and uranium. The samples consisted of step wedges of about four steps each, with individual thicknesses of about 25 to 50 microns for the heavy elements and 100 to 150 microns for the light ones. Several back emission electron radiographs were taken at various voltages. After subtracting the surrounding background density, the highest photographic density values at regions of one spectroscopic plate in contact with the elements are: aluminum—0.01, nickel—0.23, copper—0.24, molybdenum—0.59, tin—0.76, tungsten—1.40, gold—1.40, lead—1.50, and uranium—1.30. A plot of photographic density against atomic number produces a fairly

smooth curve except in the case of the gold and uranium samples used.

It is obvious that no simple correlation exists between the atomic number of a particular sample and the photographic density it produces by electron emission. Film and processing characteristics, X-ray scattering, thickness of the specimen, and other factors (see Section II A) tend to preclude an absolute analysis, but, in most instances, will permit identification of elements widely separated in atomic number when samples of those elements are known to exist in the macro-structure. Therein lies one of the major advantages of electron back emission radiography.

## VI. SUMMARY

The two electron radiographic methods may be summarized by comparing them with analogous photographic and X-ray techniques as follows:

	PHOTOGRAPHY	BACK EMISSION ELECTRON RADIOGRAPHY	TRANSMISSION ELECTRON RADIOGRAPHY	LOW-VOLTAGE X RADIOGRAPHY
Radiation Medium Used	Visible (or ultra viol.) light	100-200 kilovolt electrons		5-30 kilovolt X rays
Contrast Obtained	Difference in light transmission	Difference in atomic numbers at surface	Difference in physical density	Difference in atomic numbers
Maximum Permissible Magnifica- tion	~1000X	~15X	~25X	~100X
Apparatus Required	Corrected lens system (high-power microscope objective)	150-250 kilovolt X-ray unit (and vacuum cassette)		Low-voltage, high-current small focal spot X-ray unit with low-absorption window (and vacuum cassette)
Advantages	High resolu- tion	Simple interpretation of specimen components  No etchant necessary	Three-dimensional view  No staining necessary	No etchant or polish neces- sary



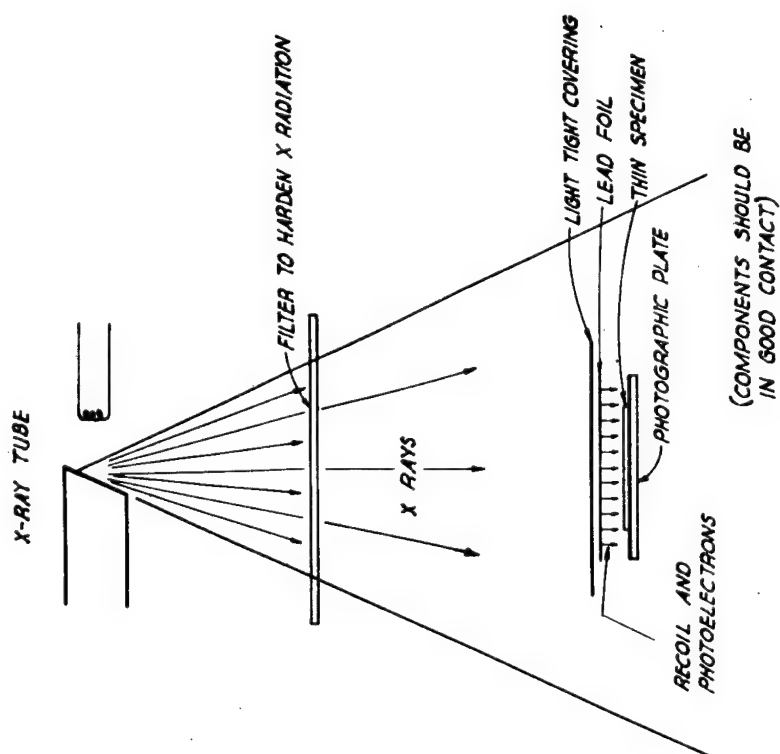


Figure 1A

## TRANSMISSION ELECTRON RADIOGRAPHY

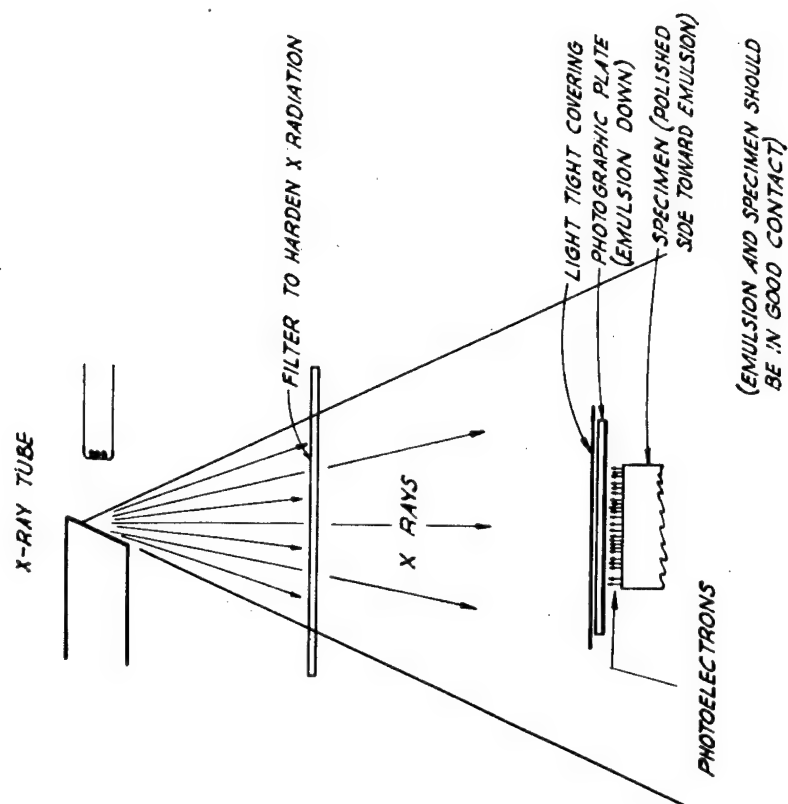


Figure 1B

## BACK EMISSION ELECTRON RADIOGRAPHY

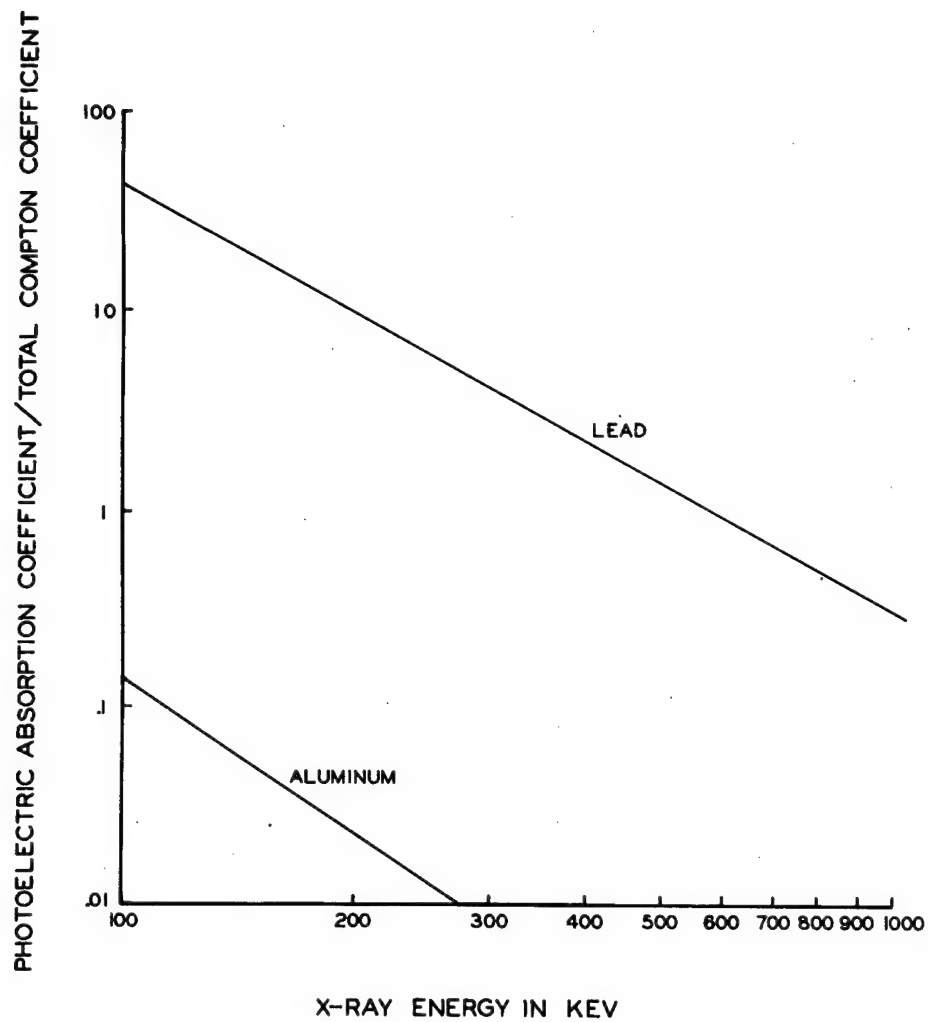
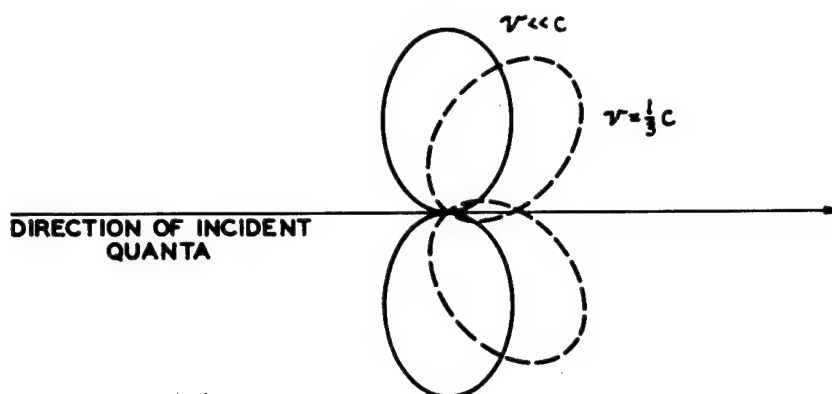


Figure 2



# INTENSITY DISTRIBUTION OF PHOTOELECTRONS

Figure 3

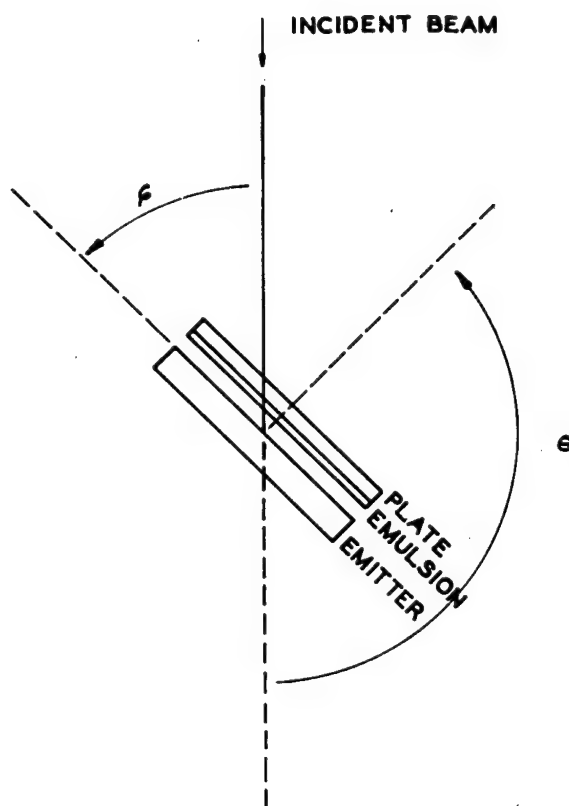


Figure 4

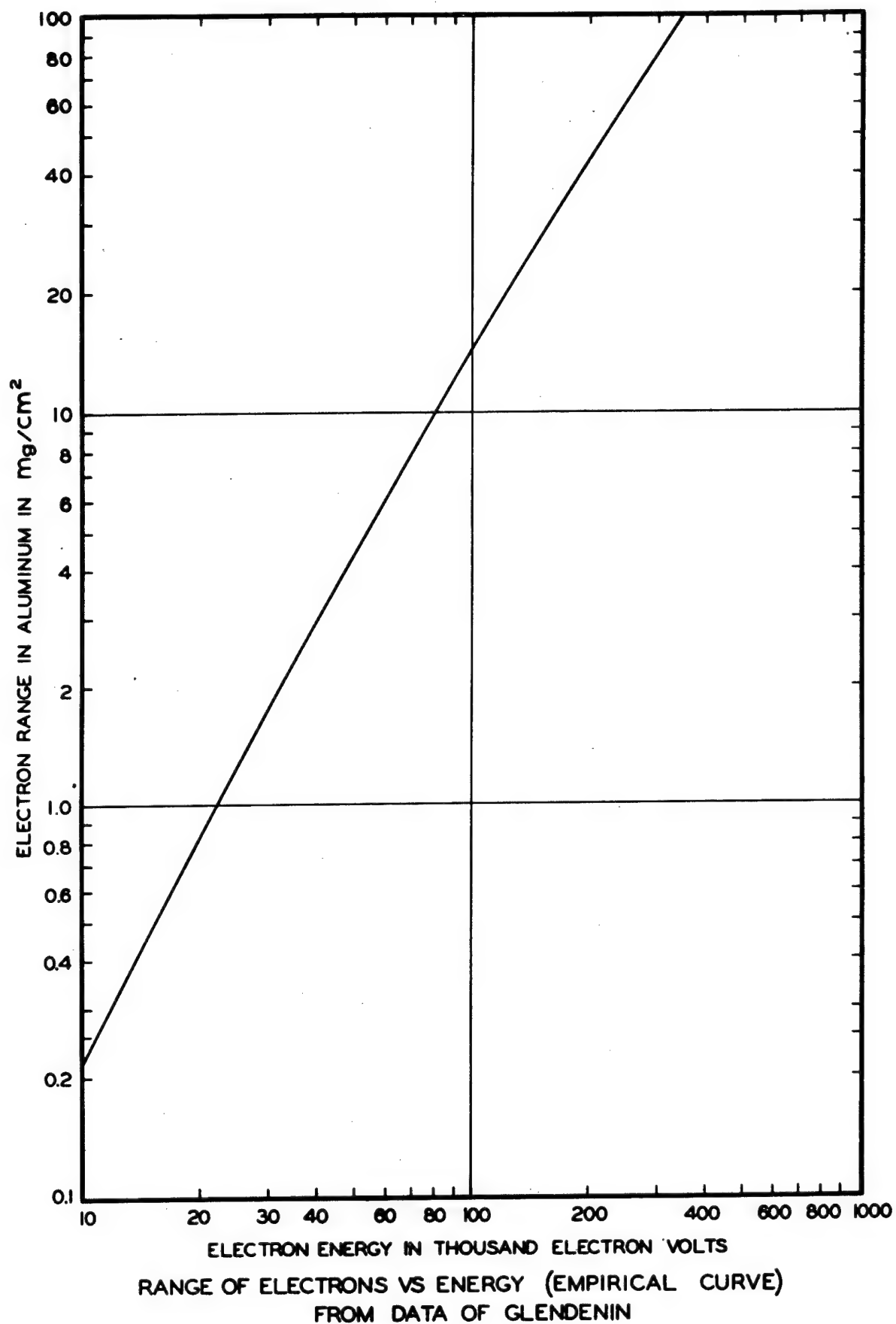
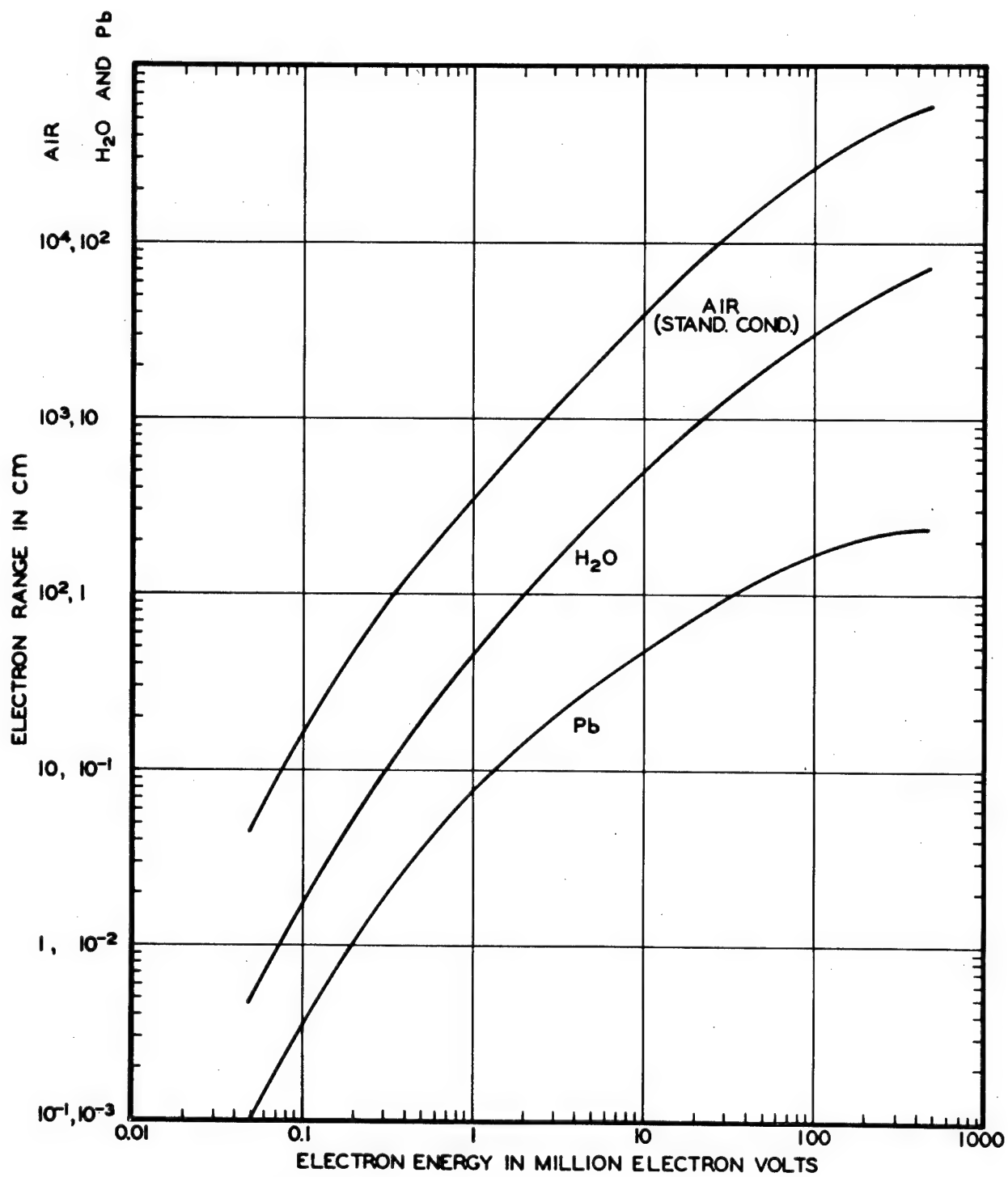
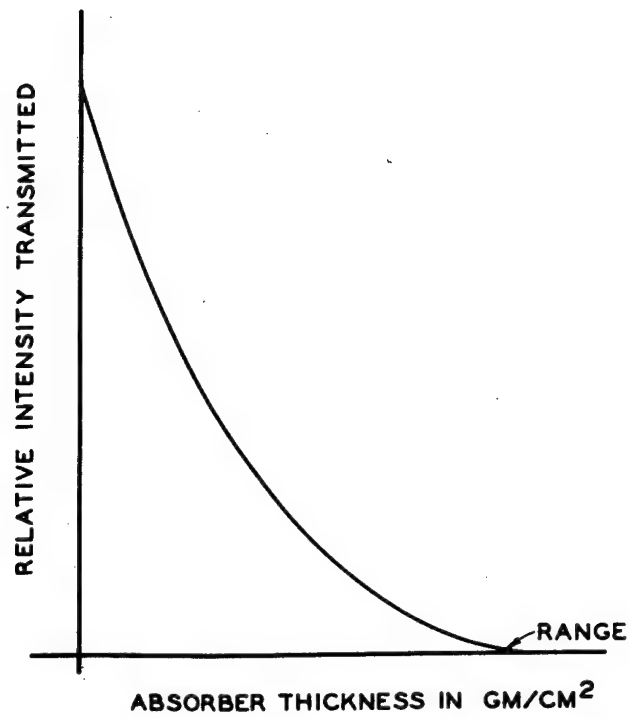


Figure 5



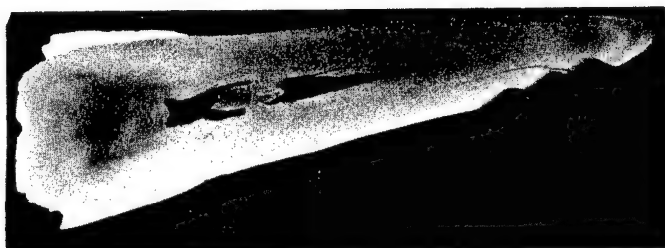
RANGE OF ELECTRONS VS ENERGY (THEORETICAL CURVE)  
ADAPTED FROM DATA OF HEITLER

Figure 6

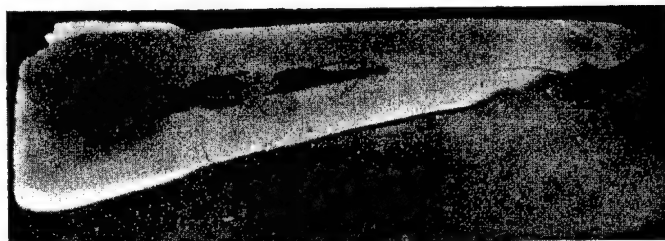


A TYPICAL ABSORPTION CURVE FOR FAST ELECTRONS

Figure 7



A X RAYS (8 PKV)



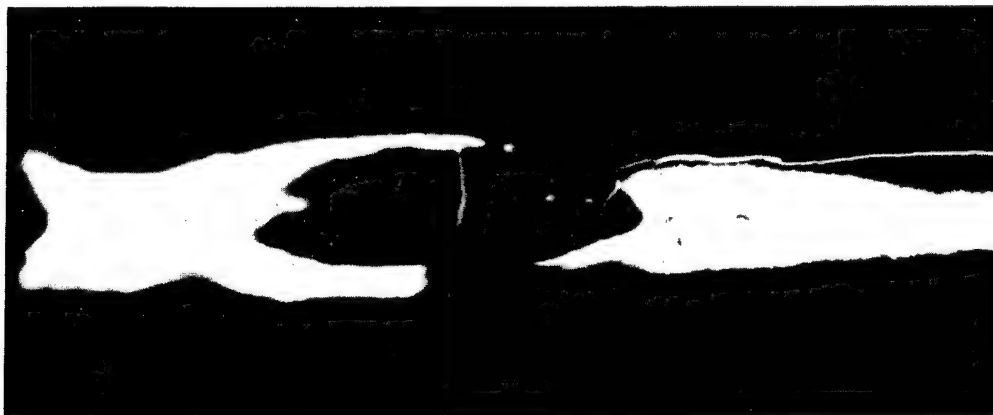
B ELECTRONS (250 PKV)



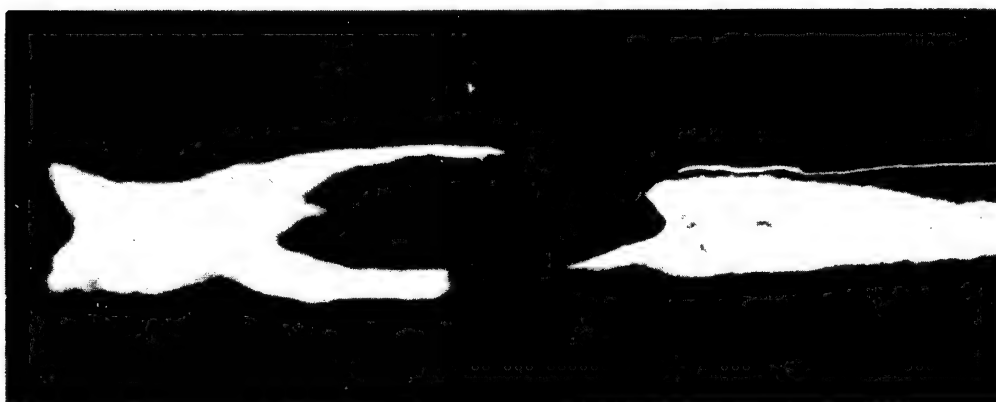
C TRANSMITTED LIGHT

Figure 8

RAT TOOTH (4.5 X)



A X RAYS (8 PKV)



B X RAYS (6.5 PKV)



C ELECTRONS (250 PKV)

Figure 9

RAT TOOTH (25 X)

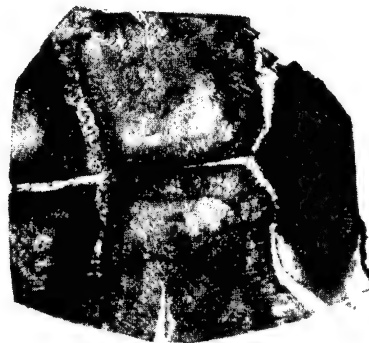




A X RAYS (12 PKV)

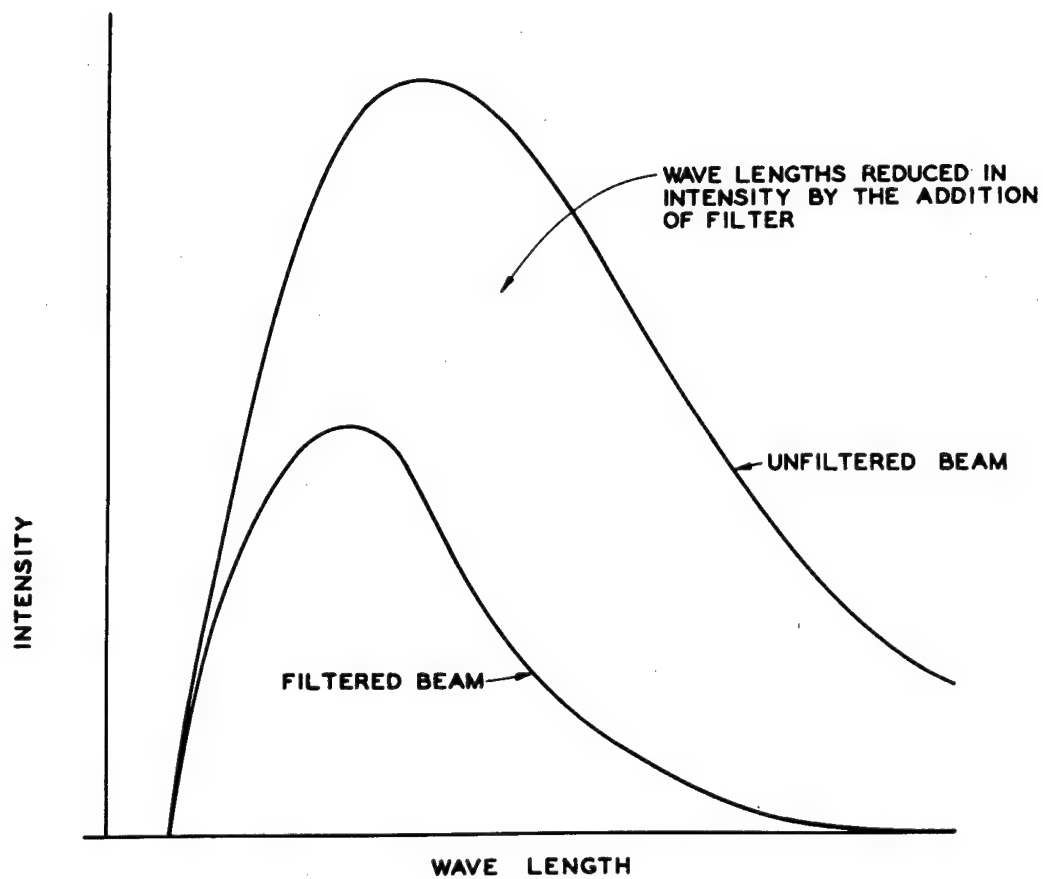


B ELECTRONS (250 PKV)



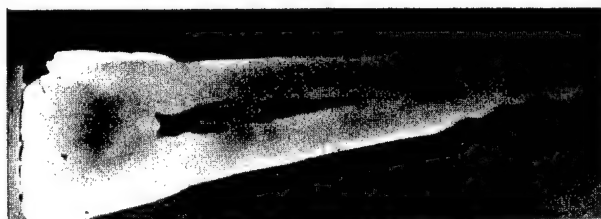
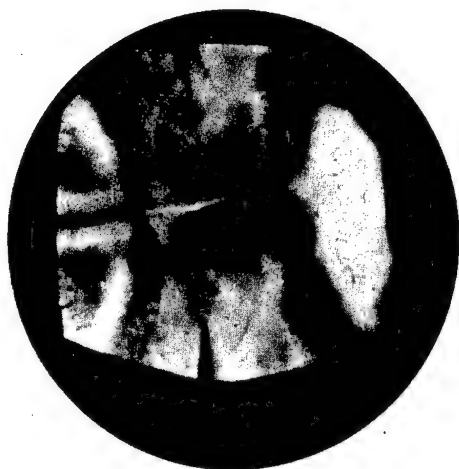
C TRANSMITTED LIGHT

Figure 10 MOUSE SKULL (4.5 X)

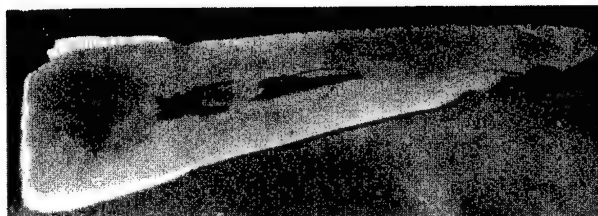


THE EFFECT OF A FILTER ON AN X-RAY BEAM

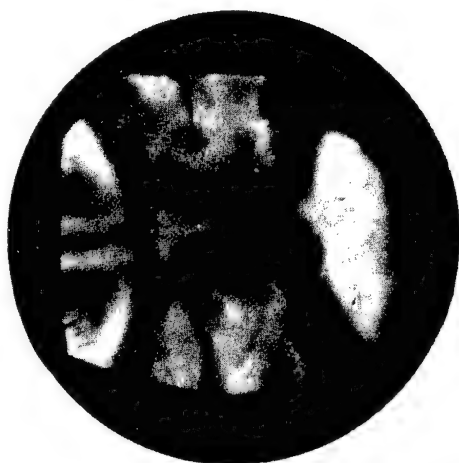
Figure 11



A 150 PKV D

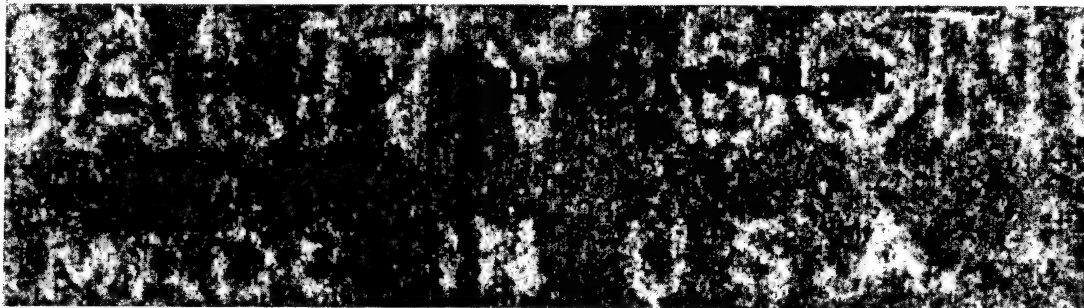


B 250 PKV E



1000 PKV F

Figure 12 ELECTRONS

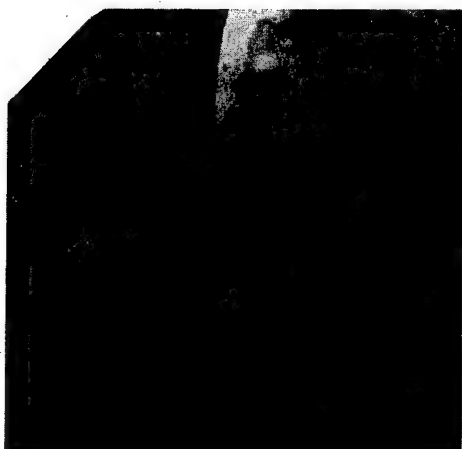


A TRANSMITTED LIGHT

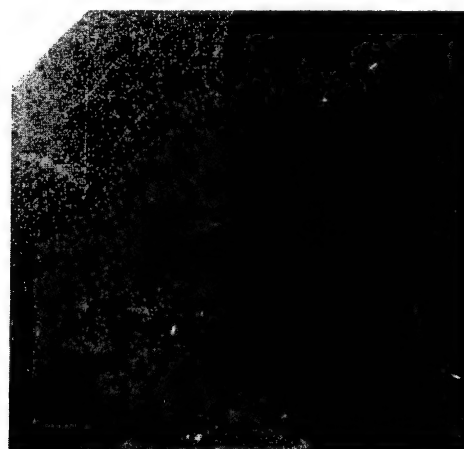


B ELECTRONS (250 PKV)

Figure 13 TYPED BOND PAPER



A ELECTRONS (250 PKV)

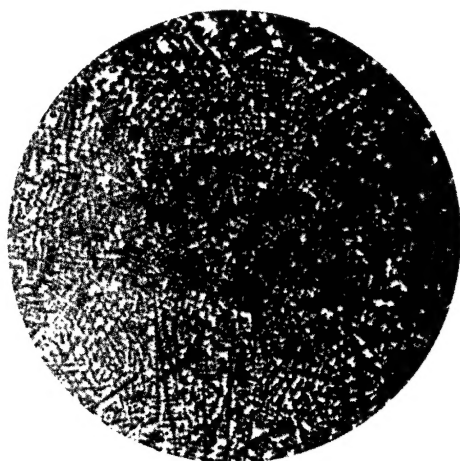


B REFLECTED LIGHT

Figure 14 BLACK PAINT



A ELECTRONS (250 PKV)



B ELECTRONS (1000 PKV)



C REFLECTED LIGHT

Figure 15 Au-Al ALLOY (3 X)

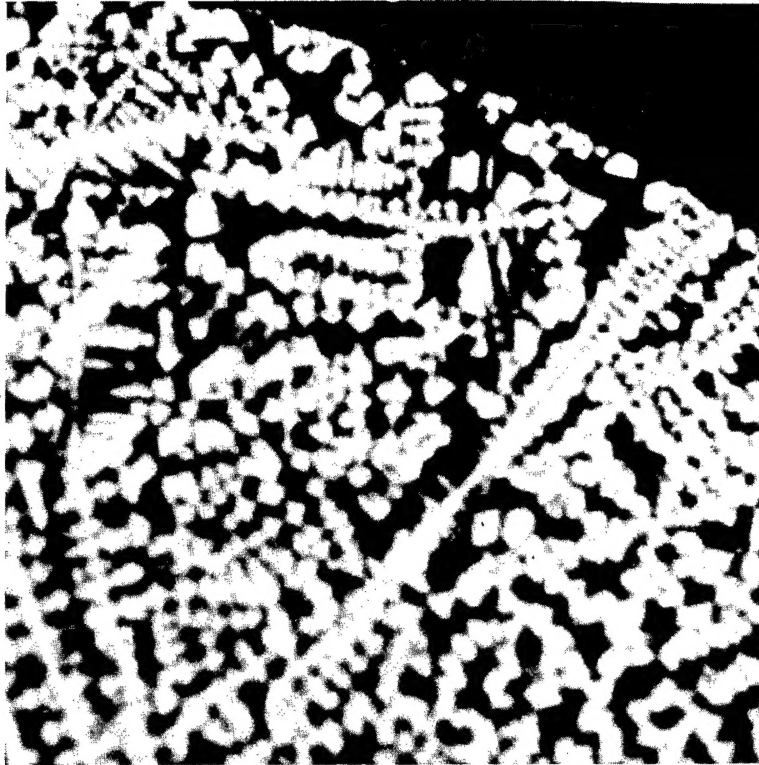
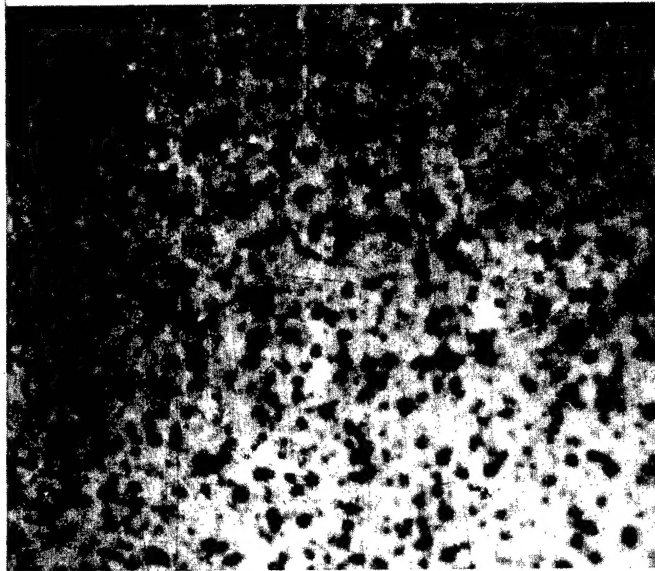


Figure 16      Au-Al ALLOY (15 X) ELECTRONS (250 PKV)



A REJECTED



B ACCEPTED

Figure 17

## REFERENCES

- <sup>1</sup>J. Trillat, J. of Appl. Phys. 19, 844 (1948);  
R. Pospisil, Non-Dest. Testing 7, 16 (Spring 1949).
- <sup>2</sup>E. Fermi, Nuclear Physics Notes (University of Chicago Press, 1950),  
p. 38.
- <sup>3</sup>E. Rutherford, J. Chadwick, and C. D. Ellis, Radiations from  
Radioactive Substances (University Press, Cambridge, 1930), p. 464.
- <sup>4</sup>W. Heitler, Quantum Theory of Radiation (University Press,  
Oxford, 1944), second edition, p. 127.
- <sup>5</sup>A. H. Compton and A. W. Simon, Phys. Rev. 25, 309 (1925).
- <sup>6</sup>W. Heitler, op. cit., p. 123; A. H. Compton and S. K. Allison,  
X Rays in Theory and Experiment (D. van Nostrand Co., New York,  
1935), p. 576.
- <sup>7</sup>W. Heitler, ibid., p. 122.
- <sup>8</sup>L. E. Glendenin, Nucleonics 2, 26 (Jan. 1948).
- <sup>9</sup>W. Heitler, op. cit., p. 223.
- <sup>10</sup>H. E. Seeman, J. of Appl. Phys. 8, 836 (1947).
- <sup>11</sup>E. Fermi, op. cit., p. 36.
- <sup>12</sup>For a report on this and other emulsions, see J. Cobb and  
A. K. Solomon, Rev. Sci. Inst. 19, 441 (1948).
- <sup>13</sup>T. Westermark, Nature 164, 1086 (1949); D. E. Beischer,  
Science 112, 535 (1950).
- <sup>14</sup>J. Trillat, op. cit., p. 847 (electron back emission radio-  
graphs in this paper were all magnified to less than ten  
diameters).

## ACKNOWLEDGEMENT

The writer expresses thanks to Mr. James W. Dutli for initiating this project, as well as for many suggestions during the work and completion of the paper; to Messrs. W. C. Herrmann and A. M. Rogers, who made the photomacrographs and reproduced the radiographs; to Mr. E. J. Davis for his drawings; to Messrs. N. C. Miller, E. H. Kalmus, and Dr. H. L. Mayer for their review of the paper; and especially to Dr. Gerold H. Tenney for making this project possible in the Los Alamos Radiographic Research Group.

END OF DOCUMENT